Vapor−Liquid−Solid Phase Transitions in Aqueous Sodium Sulfate and Sodium Carbonate from Heat Capacity Measurements near the First Critical End Point. 2. Phase Boundaries

Vladimir M. Valyashko,[†] Ilmutdin M. Abdulagatov,*[,‡,§] and Johanna M. H. Levelt Sengers[||]

N. S. Kurnakov Institute of General and Inorganic Chemistry, Russian Academy of Sciences, Moscow, SU 117907, Russia, Guest Scientist, National Institute of Standards and Technology, Boulder, Colorado 80303, Institute for Geothermal Problems of the Dagestan Scientific Center of the Russian Academy of Sciences, 367030 Makhachkala, Kalinina 39 A, Dagestan, Russia, and National Institute of Standards and Technology, 100 Bureau Drive, Stop 8380, Gaithersburg, Maryland 20899-8380

The constant volume, constant composition heat capacity data for aqueous sodium sulfate show several interesting features: one peak or step when solid salt first precipitates and, on further heating, a λ-shaped peak when the vapor- or liquid-phase disappears. These features are interpreted in terms of the solid−liquid−vapor phase diagram, and their consistency is shown with earlier *PVTx*, phase boundary, and three-phase data from the literature. New data are presented on the density of liquid solutions saturated with respect to the vapor. New liquid compositions or densities supplement the three-phase data available in the literature, and new fluid densities are reported near the critical end point. For aqueous Na_2SO_4, we find $T_{cep} = (648.2 \pm 0.2)$ K, and for aqueous Na_2CO_3, $T_{cep} = (649.0 \pm 0.2)$ K. The present heat capacity data, as well as recent data for aqueous sodium carbonate, have sufficient resolution to distinguish, for the first time, the temperature of the critical end points in aqueous sodium sulfate and aqueous sodium carbonate from the critical temperature of pure water, $T_c = (647.1 \pm 0.1)$ K.

Introduction

This paper is concerned with the high-temperature phase behavior of aqueous solutions of sodium sulfate and, to a lesser extent, sodium carbonate, as derived from recent measurements of the isochoric heat capacities of these systems by Abdulagatov et al.[1,2] We interpret these features in terms of the solid−liquid−vapor phase diagram and show their consistency with earlier *PVTx*, phase boundary, and three-phase data from Khaibullin and Novikov.[3,4] These data are referred to as Kh[3,4] data. Aqueous sodium sulfate has a complex phase diagram. Étard[5] first showed that the solubility of sodium sulfate in water begins to decrease above 250 °C. Smits and Wuite[6] measured the temperature−composition diagram in a quartz Cailletet tube up to 365 °C (Figure 1). Stable and metastable hydrated forms exist up to 32.4 °C. Rhombic and monoclinic anhydrous phases exist at higher temperatures. Above 250 °C, in the range of declining solubility that is of interest in this paper, the solid salt exists in the dehydrated form S_M only. The solid phase extends above the critical point of water, thus cutting off the salt−water critical line in a critical end point. This so-called Type-2 solid−liquid−vapor phase behavior, typical for sodium sulfate, sodium carbonate, and many other salts poorly soluble in water, will be described in more detail in the next section. Sharygin et al.[7] report indications that hydrolysis occurs at low pressures and high temperatures. This issue is not addressed in the present paper.

Comprehensive *PVTx* studies by Kh[3,4] have given much detail of the high-temperature phase behavior and density of the liquid salt solution in the presence of the vapor. From these studies, they derived the location of the three-phase line (gas−liquid−solid) and the densities and compositions of the liquid and vapor on this line. In addition, they give limited information on the density and composition of the vapor phase in the presence of the solid near and above the critical point of water.

It is the purpose of this paper to interpret the locations of the phase boundaries encountered from 350 K up to the critical end point, as they manifest themselves in peaks and jumps in the heat capacity data for aqueous sodium sulfate.[1] We also analyze data near the critical end point of aqueous sodium carbonate.[2] Satisfactory consistency with Khaibullin's *PVTx* data for the saturated liquid and for the three-phase line of aqueous sodium sulfate is demonstrated. The heat capacity data extend beyond the range of the three-phase data of Kh.[3,4] Thus, for the first time, the near vicinity of the critical end point is explored. The resolution of the C_{vx} data is high enough to distinguish the critical end point location from that of the critical point of water. Critical end point temperatures are given for both aqueous sodium sulfate and aqueous sodium carbonate.

Solids in Equilibrium with Supercritical Fluids: The Phase Diagram

Buechner[8,9] and Smits,[10−12] members of the school of van der Waals, showed at the beginning of the 20th century that there are two main types (Type-1 and Type-2) of binary systems in which solids coexist with supercritical fluid phases. The phase diagrams of these types are distinguished by the presence, or absence, of a critical end point

* To whom correspondence should be addressed at NIST, Boulder, CO.
[†] Russian Academy of Sciences.
[‡] Guest Scientist, National Institute of Standards and Technology.
[§] Institute for Geothermal Problems of the Dagestan Scientific Center of the Russian Academy of Sciences.
[||] National Institute of Standards and Technology.

10.1021/je000123z CCC: $19.00
Published on Web 10/04/2000

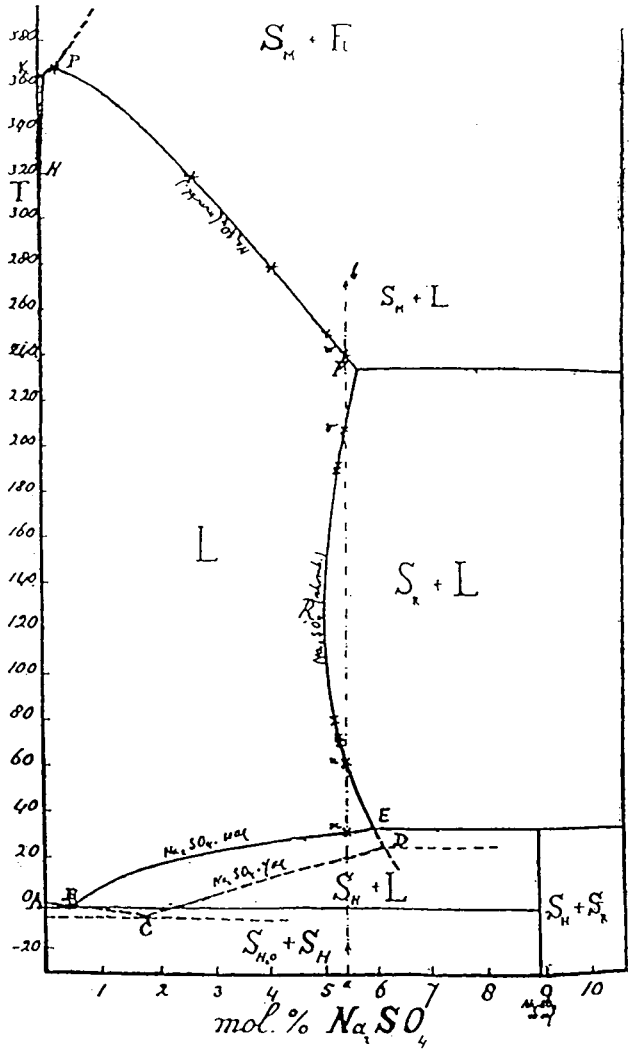

Figure 1. Phase boundaries in the temperature−composition diagram of solid and fluid aqueous sodium sulfate up to the critical point of water, taken from the original paper of Smits and Wuite.[6] The abscissa is the temperature in degrees Celcius, and the ordinate is the mole percent of Na_2SO_4 in solution. Solid phases are indicated by S, L denotes a liquid, and F denotes a supercritical fluid phase. S_H denotes solid $Na_2SO_4 \cdot 10H_2O$, S_r the rhombic anhydride, and S_m the monoclinic anhydride. Dashed curves indicate transitions to metastable phases. On the vertical line a−b, at 5.4 mol %, the solid-phase melts at 31 °C. Another solid phase appears at 61 °C, to disappear in a retrograde fashion at 206 °C. Finally, a third solid phase appears at 241 °C.

(L = G−S) at the intersection of the critical curve (L = G) and the three-phase solubility curve (L−G−S).

In binary systems, equilibrium between the solid and supercritical fluid phases arises when the nonvolatile component has a melting temperature higher than the solvent's critical temperature. A prime example is the class of water−salt systems, with water the volatile component.

For Type-1 solid−fluid phase behavior, the solubility curve does not reach all the way up to the critical curve, and a two-phase liquid−vapor region separates the two curves. In the *P*−*T* diagram, the three-phase line (L−G−S) rises to a maximum, which remains below the critical line and ends at the triple point of the pure salt. The solubility of the nonvolatile component increases monotonically with increasing temperature. Thus, there is a positive temperature coefficient of solubility. Highly soluble salts such as the alkali chlorides fall in this class. For these, the binary fluid-phase diagram is of Type-I in the classification of Van Konynenburg and Scott,[13] but there are many examples for which additional fluid−fluid immiscibility occurs.

For Type-2 solid−fluid phase behavior, the solubility of the nonvolatile (salt) component starts declining before the critical temperature of the solvent is reached. Increasingly, the composition and density of the solid-saturated liquid and vapor approach each other until a liquid−vapor critical point is reached in the presence of the solid. This is the first critical end point (L = G−S), the intersection of the critical line (L = G) and the three-phase solubility curve (L−G−S) near the critical point of the pure solvent. The (L−G−S) line originating from the triple point of the nonvolatile component intersects the (L = G) critical line originating from the critical point of the nonvolatile compound at a second critical end point, which occurs at higher temperatures, pressures, and concentrations of the nonvolatile components. The supercritical fluid−solid equilibria exist in a temperature range between the first and second critical end points, effectively cutting out the whole center of the fluid phase diagram. In these cases, the underlying fluid phase diagram is, as far as one can tell, of Type III, IV, or V binary fluid phase behavior,[13] with a (L = G) critical line interrupted by a three-phase L1−L2−G region; this region is, however, masked by the solid phase.

Alkali sulfates (Li_2SO_4, Na_2SO_4, K_2SO_4, $KLiSO_4$) and carbonates (Li_2CO_3, Na_2CO_3) belong to the Type-2 solid−fluid phase behavior. The direction of the high-temperature part of the *T*−*x* critical line is not toward the water critical point. This is a strong indication that the critical line is indeed interrupted in the underlying binary fluid phase diagrams and that there is metastable fluid−fluid immiscibility in the region hidden by the intrusion of the solid phase, as shown by Valyashko.[14,15] The system Na_2SO_4 + H_2O was the first water−salt system found to be of this type.[6]

More complex solid−fluid phase behavior can occur when this fluid−fluid phase separation is not completely masked by the solid phase. For detail, we refer to Valyashko[14] and to Peters.[16]

The Type-2 solid−fluid phase diagram of interest here is drawn schematically in the vicinity of the first critical end point in *P*−*T*, *P*−*x*, *T*−*x*, and *ρ*−*T* coordinates in Figure 2. It should be stressed that, in water−salt systems of this type, the water critical point, the critical line, and the critical end point are so close together that, up to now, they had never been resolved by experiment.

Phase Transitions on Isochoric Heating

A typical isochore is shown in Figure 3. It is clear that several events occur when the sodium sulfate solution is heated isochorically. Two peaks or jumps in the isochoric heat capacity are often found. The sharp changes of measurable properties are connected with fluid−fluid and fluid−solid-phase transitions occurring in a binary mixture heated in a closed volume.

In the case of a binary water−salt system of Type-2, heating the liquid solution in equilibrium with a vapor can lead to four different sequences of phase transitions, depending on the fill coefficient or the average fill density and on the salt concentration in the initial mixture.

(The fill coefficient equals the ratio of the volume of the solution to the volume of the vessel at ambient temperature. The average density equals the ratio of the mass of solution to the volume of the vessel at ambient temperature. A sequence of experimental data on the heat capacity of the multiphase system obtained for a given average

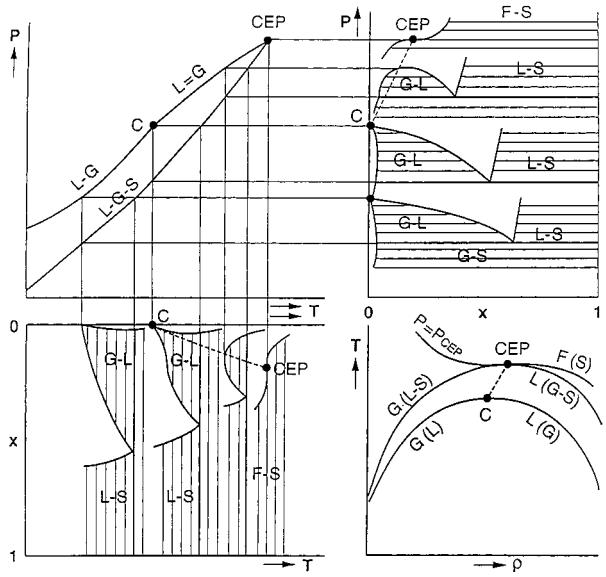

Figure 2. Schematic of the Type-2 solid−fluid phase diagram in the vicinity of the water critical point, *C*, and the first critical end point, CEP. Shown are a $P-T$ projection, constant-T sections in $P-x$ space, constant-P sections in $T-x$ space, and a temperature−density diagram in which the coexistence curve for pure water is drawn, as well as the coexistence curve for the salt-saturated solution near the critical end point. Note that CEP is at the top and that the salt-saturated isobar through the critical end point has a horizontal tangent.

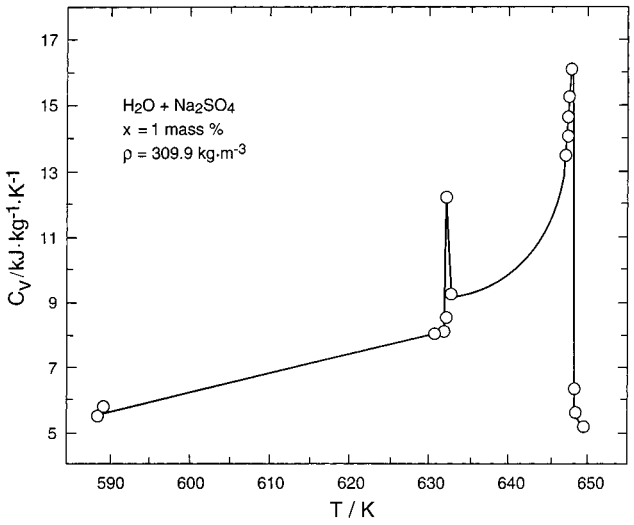

Figure 3. Typical C_{vx} behavior as a function of temperature along an isochore.

density will be called an isochore, even though the volume occupied by the solution is not strictly constant during an experimental run, due to the thermal expansion of the calorimeter vessel and the varying volume of the solid.)

1. At the highest average densities, the liquid phase expands on heating and fills the entire vessel, while the vapor phase disappears. A transition (L−G ⇔ L) occurs, with a drop in heat capacity as the number of phases decreases.

2. At low fill density, and at very low salt concentration of the initial mixture, heating increases the vapor density and the concentration of salt in the steam, resulting in disappearance of the liquid. A transition takes place from two- to one-phase equilibrium (L−G ⇔ G), again with a drop in heat capacity.

3. On being heated at intermediate average densities higher than critical, and before the thermal expansion causes the liquid to fill the entire volume, the initially unsaturated liquid solution becomes saturated with salt due to the negative temperature coefficient of solubility typical for systems of Type-2. In this case, the first phase transformation is the crystallization of solid from the liquid solution in equilibrium with its vapor, (L−G ⇔ L−G−S), with an increase in heat capacity as the number of phases increases. On further heating of the mixture, the concentration of the saturated liquid solution along the solubility curve decreases. Finally, the expanding liquid fills the cell save for the volume occupied by the solid salt. A transition from (L−G−S ⇔ L−S) equilibrium takes place, with a decrease in heat capacity.

4. If the average fill density is somewhat lower than critical, the first transition is the appearance of solid salt, (L−G ⇔ L−G−S), with the heat capacity increasing. At higher temperatures, a second transition will correspond to disappearance of the liquid phase, a transformation of three-phase to two-phase (L−G−S ⇔ G−S) equilibrium, with a decrease in heat capacity.

Cases 1, 3, and 4 have been encountered in the experimental data of Abdulagatov et al.[1]. The first kind, (L−G ⇔ L), is seen in the isochores at 664.0 kg·m^{-3} and 860.5 kg·m^{-3} for 1 mass %; 925.9 kg·m^{-3} for 5 mass %; and 830.7 kg·m^{-3}, 844.8 kg·m^{-3}, 936.3 kg·m^{-3}, 986.2 kg·m^{-3}, 1059.0 kg·m^{-3}, and 1072.5 kg·m^{-3} for 10 mass % Na_2SO_4. The third kind, (L−G ⇔ L−G−S) followed by (L−G−S ⇔ L−S), is found in the isochores at 361.9 kg·m^{-3} and 521.3 kg·m^{-3} for 1 mass % Na_2SO_4; at 490.0 kg·m^{-3} and 674.7 kg·m^{-3} for 5 mass %; and at 537.6 kg·m^{-3}, 697.8 kg·m^{-3}, 774.2 kg·m^{-3}, and 792.2 kg·m^{-3} for 10 mass % Na_2SO_4. The fourth kind, (L−G ⇔ L−G−S) followed by (L−G−S ⇔ G−S), is present on the isochores with average densities of 250.1 kg·m^{-3} and 309.9 kg·m^{-3} for 1 mass % Na_2SO_4.

The above description has referred to jumps in heat capacity to be expected when boundaries are crossed. The appearance of a typical intermediate-density isochore, however, shows two *peaks* rather than two jumps (Figure 3). The first peak, well below the water critical temperature of 647 K, marks the appearance of the solid phase. For an equilibrium phase transition, an upward jump would be expected in the heat capacity. In our interpretation, for which we will give evidence in the next section, the nucleation of the new phase is retarded until the sample reaches a temperature about 1 K beyond the three-phase temperature. The first peak is caused by the sudden absorption of heat as the system relaxes to the three-phase state. The second peak is seen when the vapor (case 4) or liquid (case 3) disappears from the cell under conditions where the fluid is close to (though not at) the critical point of steam and close to the critical end point. Though not strictly critical, the system is close enough to a critical-point phase transition to display the λ-shaped heat capacity anomaly typical of the weakly diverging C_v of pure fluids.

This last point is not as obvious as it may seem. First of all, the present mixture will not reach a critical point unless it would be exactly at the concentration and density of the critical end point. Since the concentrations and densities were arbitrarily chosen, this is unlikely. Furthermore, as is well-known, the heat capacity divergence is suppressed in a binary mixture of constant volume and composition: more than one "density-like" variable, in the language of Griffiths and Wheeler[17] and of Anisimov et al.,[18] is kept constant. The suppression is particularly fast when the two components are very unlike, as is the case here. This argument, however, does not pertain to the present case, because the excess salt keeps one "field" variable, a

chemical potential, virtually constant. Thus, a weak divergence of the isochoric heat capacity may be expected at the critical end point. It is therefore understandable that a λ-shaped peak appears on isochores that pass near the critical end point. Furthermore, the present data suggest that the addition of an electrolyte to water near its critical point does not change the nonclassical nature of the criticality: the weak divergence of the isochoric heat capacity typical of pure water appears to be retained.

Appearance of a Solid Phase in Liquid−Vapor Conditions

In attributing observed peaks or jumps in the $C_{vx}-T$ curve to a particular type of phase transition, use was made of existing information on the solubility curve or on the three-phase curve: namely, data on the concentration of the liquid solution saturated with salt while in equilibrium with vapor, published by Kh[3,4] and by others; see the compilation by Zdanovsky et al.[19] The data by Abdulagatov et al.[1,2] analyzed here were reported on the ITS-90 temperature scale. The temperatures reported by Kh,[3,4] and in the Zdanovsky et al.[19] compilation, were mostly recorded on the IPTS-48 and IPTS-68 scales. The temperature uncertainty of those older data is generally 0.1 K at the very best. Since the difference between the scales is only 0.044 K at the critical point of water, we have decided not to convert the older data to ITS-90.

If conditions are such that on isochoric heating of the liquid−vapor system a solid phase is formed (case 3 in the previous section, first peak) then an upward *jump* in heat capacity would be expected. This jump should occur at a temperature somewhat *lower* than the three-phase temperature that would correspond to the composition of the liquid solution filled into the calorimeter. This is so because, on heating, water evaporates from the liquid solution, forming a coexistent vapor phase that is virtually pure water of increasing density. Thus, the liquid solution becomes more concentrated, and the solubility curve is reached at a lower temperature than if the liquid phase had kept its initial composition.

In fact, however, the heating curves show *peaks* about 1 K *higher* than the three-phase temperature corresponding to the fill composition of the liquid. These peaks must be due to superheating preceding the formation of a solid critical-size nucleus. This hypothesis was confirmed by traversing the temperature region around the peak in both the heating and the cooling modes on a few of the isochores. The data for three isochores are given in Table 2 of Abdulagatov et al.,[1] at 10 mass %, and at densities of 537.6 kg·m^{-3}, 697.8 kg·m^{-3}, and 774.2 kg·m^{-3}. In the cooling mode, marked by superscript C, no peak is observed, and the phase transition occurs about 1 K below the peak observed on heating; see Figure 4. The total energy needed to heat the calorimeter from a temperature well below to one well above the transition must be identical to the heat extracted in the reverse process. Therefore, the excess area under the peak must equal the excess area under the jump; Figure 4 appears to be consistent with this first-law requirement to within the admittedly rather large uncertainty in how the peak is drawn through the data points. The jump in the curve in the cooling mode is taken as the mark of the phase transition.

This interpretation of the heating−cooling curves makes it possible to correct for supersaturation those isochores for which only a heating run was made. We draw the peak as well as possible, estimate its area, and do an equal-area construction of the jump the C_{vx} curve would have made under equilibrium conditions; see Figure 5. In this way,

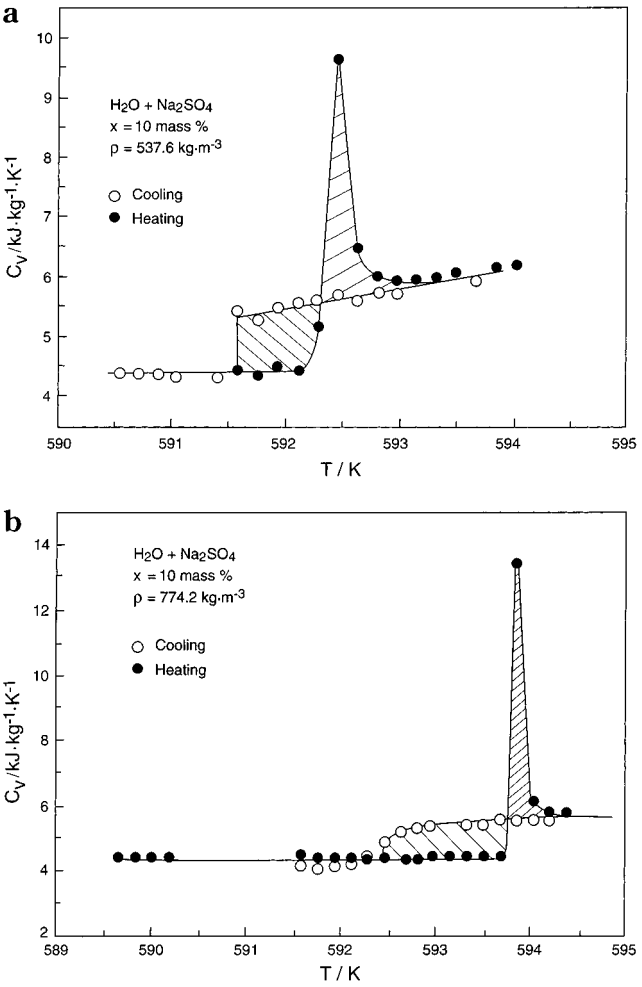

Figure 4. (a and b) Heat capacities measured in a heating and cooling mode. In the heating mode, hysteresis occurs prior to nucleation of the solid phase.

for the solid phase on nine different isochores, the equilibrium temperatures of precipitation are obtained. These transitions are the ones listed with superscript *a* in Table 1. The uncertainties in the transition temperatures of these nine isochores were estimated from the largest variations obtained by drawing the peak in question in different ways.

In Table 1, all other transition temperatures observed in Abdulagatov et al.[1] are listed. Those are the ones in which a vapor phase disappears in the absence of salt and the ones in which a fluid phase disappears in the presence of salt. In these cases, the heat capacity drops, and there is no superheat. The uncertainty indicated corresponds to half the distance, in K, between the last point before and the first point after the jump. In the prescription by Taylor and Kuyatt,[20] the uncertainty given in Table 1 would correspond to $\sigma\sqrt{3}$, with σ one standard deviation.

Volume of the Calorimeter

It is necessary to know the volume of the calorimeter, $V(T,P)$, at a temperature T and pressure P, for the purpose of calculating densities of phases. The volume of the calorimeter at T, or at P, was calculated from

$$V(P,T) = V_0 + \Delta V_P + \Delta V_T$$

$$\Delta V_P/\mathrm{cm}^3 = (1.555 \times 10^{-5}) V_0 (P/\mathrm{MPa} - 0.1)$$

$$\Delta V_T/\mathrm{cm}^3 = (5.160 \times 10^{-5}) V_0 (T/\mathrm{K} - 293.15) \qquad (1)$$

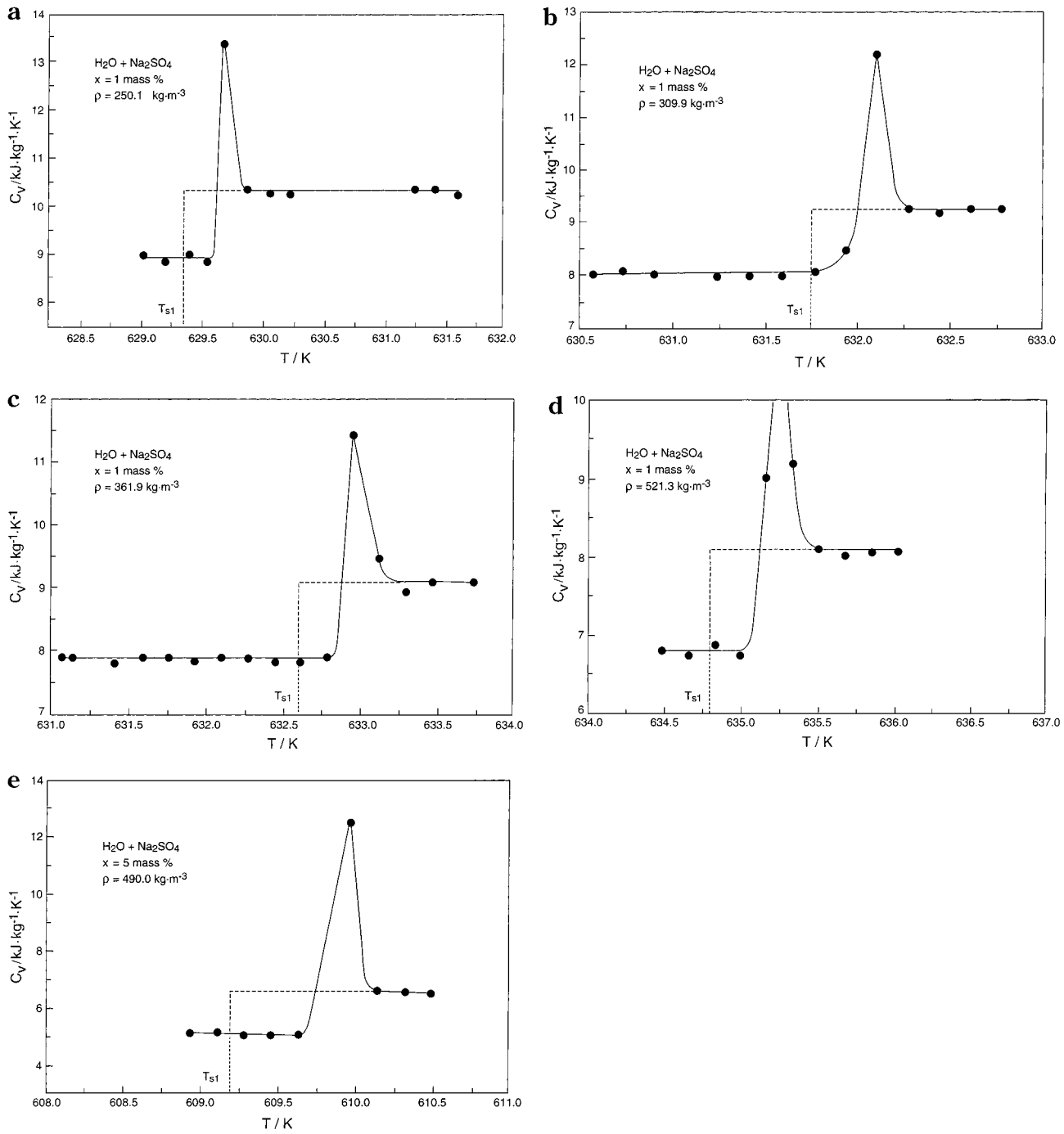

Figure 5. (a−e) Equal-area construction in order to correct for overshoot of the phase transition in the heating mode.

Here V_0 is the volume of the calorimeter, 101.45 cm^3, at a pressure of 0.1 MPa and a temperature of 293.15 K. The temperature expansion was obtained from the known expansion coefficient of the calorimeter material. The pressure expansion was obtained by calibration. The volume at ambient conditions is known to 0.015%, and the fill mass to 0.005%. The uncertainty of the pressure correction is estimated to be about 10%, and that of the temperature correction, to be about 1.5%. At the critical point of water, eq 1 gives for the pressure correction 0.034% of the volume, with an uncertainty of 0.0034%. Equation 1 gives for the temperature correction 1.8% of the volume, with an uncertainty of 0.027%. Consequently, the uncertainty in the volume expansion at the water critical point would be 0.003% + 0.027% = 0.03%. Adding in the uncertainty at ambient conditions, a conservative estimate of the volume uncertainty is 0.05% at all T, P in this experiment.

Disappearance of a Fluid Phase in the Absence of Solid

As mentioned earlier, case 1, the simple liquid−vapor to liquid-phase transition in the absence of solid salt is encountered on nine isochores in Table 2 of Abdulagatov et al.,[1] at the higher densities. For isochores from 830.7 kg·m^{-3} to 1072.5 kg·m^{-3} at 10 mass % Na_2SO_4, at 925.9 kg·m^{-3} for 5 mass %, and at 664.0 kg·m^{-3} and 860.5 kg·m^{-3} for 1 mass %, only one phase transition is observed (Table 1). It occurs at temperatures well below those at which a solid phase should first appear in a liquid−vapor system of the given composition. Moreover, the heat capacity *decreases* on passing through the transition while heating.

Table 1. Phase Transition Temperatures Derived from the Experimental C_{vx}−T Data on Various Isochore−Isopleths for Aqueous Na_2SO_4 Solutions

	T/K	
avg density/kg·m^{-3}	first peak or jump in C_{vx}	second peak or jump in C_{vx}
	1 mass % Na_2SO_4	
250.1	629.34[a] ± 0.10 (L−G ⇔ L−G−S)	647.42 ± 0.35 (L−G−S ⇔ G−S)
309.9	631.76[a] ± 0.20 (L−G ⇔ L−G−S)	648.12 ± 0.17 (L−G−S ⇔ G−S)
361.9	632.60[a] ± 0.10 (L−G ⇔ L−G−S)	647.95 ± 0.17 (L−G−S ⇔ L−S)
521.3	634.80[a] ± 0.10 (L−G ⇔ L−G−S)	638.24 ± 0.17 (L−G−S ⇔ L−S)
664.0	600.29 ± 0.18 (L−G ⇔ L)	
860.5	493.03 ± 0.10 (L−G ⇔ L)	
	5 mass % Na_2SO_4	
490.0	609.16[a] ± 0.35 (L−G ⇔ L−G−S)	644.45 ± 0.09 (L−G−S ⇔ L−S)
674.7	609.66[a] ± 0.15 (L−G ⇔ L−G−S)	615.83 ± 0.17 (L−G−S ⇔ L−S)
925.9	461.05 ± 0.11 (L−G ⇔ L)	
	10 mass % Na_2SO_4	
537.6	591.46[a] ± 0.17 (L−G ⇔ L−G−S)	643.02 ± 0.16 (L−G−S ⇔ L−S)
697.8	592.16[a] ± 0.10 (L−G ⇔ L−G−S)	619.62 ± 0.19 (L−G−S ⇔ L−S)
774.2	592.26[a] ± 0.16 (L−G ⇔ L−G−S)	603.58 ± 0.17 (L−G−S ⇔ L−S)
796.2	no data	598.55 ± 0.17 (L−G−S ⇔ L−S)
830.7	587.82 ± 0.09 (L−G ⇔ L)	
844.8	579.71 ± 0.05 (L−G ⇔ L)	
936.3	516.59 ± 0.09 (L−G ⇔ L)	
986.2	469.19 ± 0.20 (L−G ⇔ L)	
1059.0	384.48 ± 0.11 (L−G ⇔ L)	
1072.5	354.29 ± 0.12 (L−G ⇔ L)	

[a] For these points, the measured peak, which occurred because of superheating, was corrected downward by an equal-area construction. The indicated uncertainties are estimated as explained in the text. The symbols in parentheses indicate the type of phase transition occurring.

Table 2. Densities of Liquid Solutions (ρ) at Vapor Pressures and in the Absence of Solid

avg density/kg·m^{-3}	T/K	ρ/kg·m^{-3}
	1 mass % Na_2SO_4	
664.0	600.29 ± 0.18	653.5 ± 0.4
860.5	493.03 ± 0.10	851.7 ± 0.5
	5 mass % Na_2SO_4	
925.9	461.05 ± 0.11	917.9 ± 0.5
	10 mass % Na_2SO_4	
830.7	587.82 ± 0.09	818.3 ± 0.6
844.8	579.71 ± 0.05	832.3 ± 0.5
936.3	516.59 ± 0.09	925.6 ± 0.5
986.2	469.19 ± 0.20	977.3 ± 0.6
1059.0	384.48 ± 0.11	1054.5 ± 0.6
1071.5	354.39 ± 0.12	1069.1 ± 0.6

Thus, the phase transition observed can mark only the disappearance of the vapor phase (L−G ⇔ L). At the phase transition, the density of the liquid solution is readily calculated from the volume of the calorimeter (see, for example, eq 1) and the mass of the solution.

For the three compositions, the densities and temperatures of the liquid solutions, and their uncertainties, are listed in Table 2. As an example, take the first point, at 1 mass %, with an average density of 664.0 kg·m^{-3} and a transition temperature of (600.29 ± 0.18) K. At this temperature, and at 12.3 MPa, the volume of the calorimeter is 103.076 cm^3, with a relative uncertainty of 0.05%. From the given fill density, the fill mass is calculated as 67.363 g, with a relative uncertainty of 0.005%. So the range of volume is from 103.129 cm^3 to 103.025 cm^3, and the range of fill mass is from 67.366 g to 67.360 g. Thus, the liquid density ranges from 0.6532 g·cm^{-3} to 0.6539 g·cm^{-3}. Table 2 shows the average, with an uncertainty of half the range.

Figure 6 shows good agreement of the present data with the density of aqueous Na_2SO_4 solutions at vapor pressure, as obtained by Kh.[4] The uncertainty of their densities, ±2 kg·m^{-3}, is 2−4 times larger than ours.

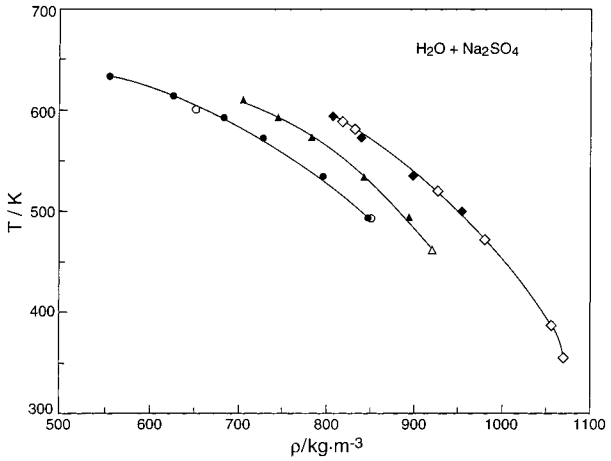

Figure 6. At three concentrations: temperature dependence of the density of the liquid in equilibrium with the vapor in the absence of solid. The solid curves are guides to the eye. 10 mass %: ◇, this work; ◆, Khaibullin and Novikov.[4] 5 mass %: △, this work; ▲, Khaibullin and Novikov.[4] 1 mass %: ○, this work; ●, Khaibullin and Novikov.[4]

Densities and Compositions of the Fluid Phases as the Solid First Appears

Cases 3 and 4, first peak, mark the entry into the three-phase condition by the appearance of solid salt. These are the data points subscripted *a* in Table 1 and labeled as 1 in Table 3. From the calorimetric experiment, only the transition temperature, the total volume $V(T,P)$, and the fill masses of water and salt are known. This is not sufficient to determine densities and compositions of individual phases. Additional information is needed to calculate the amounts and the properties of the fluid phases. Kh[3,4] measured the temperature, pressure, and densities of coexisting phases. From these, they derived the liquid and vapor densities, temperature, and pressure at various liquid compositions on the three-phase line.

Table 3. Composition and Density of Liquid and Vapor Solutions at Three-Phase Equilibrium

avg density (kg·m^{-3})/ init conc (mass %)/peak no.		liquid solution		vapor solution		
	T/K	x/mass %	ρ/kg·m^3	x/mass %	ρ/kg·m^3	P_S/MPa
537.6/10/1	591.46 ± 0.17	10.47 ± 0.02	823 ± 2[a]	0	61.3−60.4[a]	10.8 ± 0.1[a]
697.8/10/1	592.16 ± 0.10	10.16 ± 0.01	819 ± 2[a]	0	61.0−62.1[a]	10.9 ± 0.1[a]
774.2/10/1	592.26 ± 0.16	10.060 ± 0.003	818 ± 2[a]	0	61.1−62.2[a]	10.9 ± 0.1[a]
796.2/10/2	598.55 ± 0.17	8.1 ± 0.8[b]	772.1 ± 5.4			11.7 ± 0.1[a]
774.2/10/2	603.58 ± 0.17	6.7 ± 0.67[b]	742.3 ± 4.5			12.6 ± 0.1[a]
490.0/5/1	609.16 ± 0.35	5.32 ± 0.02	707 ± 2[a]	0	79.5−83.2[a]	13.4 ± 0.1[a]
674.7/5/1	609.66 ± 0.15	5.040 ± 0.004	704 ± 2[a]	0	80.5−84.2[a]	13.5 ± 0.1[a]
674.7/5/2	615.83 ± 0.17	3.5 ± 0.35[b]	655.7 ± 2.2			14.8 ± 0.1[a]
697.8/10/2	619.62 ± 0.19	2.8 ± 0.28[b]	647.5 ± 2.2			15.6 ± 0.1[a]
250.1/1/1	629.34 ± 0.10	1.66 ± 0.03	577 ± 2[a]	0	128.7−131.9[a]	17.7 ± 0.1[a]
309.9/1/1	631.76 ± 0.20	1.37 ± 0.03	562 ± 2[a]	0	135.4−138.6[a]	18.2 ± 0.1[a]
361.9/1/1	632.60 ± 0.10	1.23 ± 0.01	556 ± 2[a]	0	137.8−141.0[a]	18.4 ± 0.1[a]
521.3/1/1	634.80 ± 0.10	1.019 ± 0.002	538 ± 2[a]	0	143.7−146.9[a]	18.9 ± 0.1[a]
521.3/1/2	638.24 ± 0.17	0.75 ± 0.08[b]	511.0 ± 0.6			19.8 ± 0.1[a]
537.6/10/2	643.02 ± 0.16	<0.3	485.4 ± 1.2			21.0 ± 0.1[a]
490.0/5/2	644.45 ± 0.09	<0.3	461.7 ± 1.0			21.4 ± 0.1[a]
361.9/1/2	647.95 ± 0.17	<0.3	352.7 ± 0.7			22.3 ± 0.1[a]
309.9/1/2	648.12 ± 0.17			<0.3	302.0 ± 0.5	22.3 ± 0.1[a]
250.1/1/2	647.42 ± 0.35			<0.3	243.7 ± 0.5	22.1 ± 0.1[a]

[a] Values obtained by interpolation of data from refs 3 and 4. The first values of vapor density were obtained from the Harvey et al. (1997) steam program[21,22] at given temperatures and vapor pressures of saturated solutions taken from refs 3 and 4. The second values of vapor density were obtained by interpolation of density data from refs 3 and 4. [b] Values obtained from the summary solubility curve.

A first estimate of the vapor density $\rho_{vap}(T,P)$ at our transition temperatures is obtained by means of the Kh[4] three-phase values of pressure and temperature, assuming that the vapor below 635 K is pure steam and using the NIST/ASME steam properties program.[21] In the present system the salt concentration in the vapor phase is negligible, namely from 1.3×10^{-9} to 2.0×10^{-8} mole fraction of Na_2SO_4 in the range from 618 K to 633 K, according to Harvey and Bellows.[22] The vapor density ρ_{vap} at our transition temperatures is obtained by interpolation of the Kh[4] three-phase data for the vapor density. These two values of the vapor density are listed in Table 3. The Kh[4] published vapor densities are systematically higher, by up to 5%, than the ones calculated for pure steam from the Kh[4] vapor pressures at our transition temperatures. In calculations to follow, the average is used, with an uncertainty of half the spread. This uncertainty is usually smaller than the ±2 kg·m^{-3} claimed by Kh[3,4] for their density measurements.

The liquid densities ρ_{liq} at our transition temperatures are obtained by interpolation of the Kh[4] densities of the three-phase line. The corresponding mass % composition of the liquid phase, x_{liq}, is then obtained by the following considerations. Call the volume occupied by the vapor V_{vap}, that by the liquid V_{liq}, the mass of salt M_{salt}, and the total fill mass M. Mass and volume balances then yield

$$\rho_{vap}V_{vap} + \rho_{liq}(V - V_{vap}) = M \qquad (2)$$

Therefore

$$V_{vap} = (\rho_{liq}V - M)/(\rho_{liq} - \rho_{vap}) \qquad (3)$$

so that

$$x_{liq}/100 = M_{salt}/\rho_{liq}V_{liq} = M_{salt}/\{\rho_{liq}(V - V_{vap})\} \qquad (4)$$

As a typical example, consider the 5 mass % data point for which the solid first appears at (609.16 ± 0.35) K. This data point is characterized by T = (609.16 ± 0.35) K, M_{salt} = 2.486 g, P_{vap} = (13.4 ± 0.1) MPa, $V(P,T)$ = (103.13 ± 0.05) cm^3, M_{water} = 47.22 g, ρ_{vap} = 0.0795 g·cm^{-3} {steam at P_{vap}(Kh),T}, M = 49.71 g, ρ_{vap} = 0.0832 g·cm^{-3} (Kh), ρ_{liq} = (0.707 ± 0.002) g·cm^{-3} (Kh), $V\rho_{liq}$ = (72.91 ± 0.2) g, $V\rho_{liq} - M$ = (23.2 ± 0.2) g, $\rho_{liq} - \rho_{vap}$= (0.627 ± 0.004) g·cm^{-3}, and V_{vap} = 37.0 ± 0.3 cm^3.

Thus, x_{liq} = 100[2.486/{0.707(103.13 − 37)}] = 5.32 mass %. The uncertainty in x_{liq} is determined by calculating x_{liq} for extreme values of ρ_{liq}, 0.705 and 0.709 g·cm^{-3}, and ρ_{vap}, 0.0795 and 0.0832 g·cm^{-3}, and is found to be ±0.002 mass %; there is substantial cancellation of errors in the contributions to eq 4.

Note, however, that, according to Kh,[4] the liquid composition at our transition temperature should be 5 mass %. In the present case, however, the liquid composition must be enriched beyond the 5% starting composition, because of the presence of a substantial amount of vapor. The discrepancy is therefore of concern. In their case, vapor and liquid densities were measured directly for a solution of known overall composition. The transition temperature was interpolated from the break in the isochore, and just as in the present case, they did correct for the mass of water present in the vapor. The 5% data point reported on the three-phase line must, however, have been the result of further interpolation of the original transition-point data, since it is impossible to estimate the ambient-temperature fill conditions that will lead to 5% concentration of the liquid phase at the three-phase line. By assuming that the Kh[4] densities are more reliable than the Kh[4] liquid compositions, we have been able to come up with more accurate compositions for the liquid on the three-phase line. Had the Kh[4] liquid compositions been assumed as correct, then calculation of the liquid density would have faced an insurmountable hurdle, namely a zero volume for the vapor.

The compositions and densities of the coexisting liquid and vapor phases when the solid first appears are given in Table 3. The nine isochores are those for which an uncertainty is stated for the composition. The uncertainties of the temperature are those given in Table 1. The uncertainties in the liquid densities for these nine isochores are those of Kh,[4] estimated to be ±2 kg·m^{-3}. The uncertainties in vapor densities at the given transition temperature are half the difference between the Kh[4] values and the density of pure steam at the Kh[4] vapor pressure. The

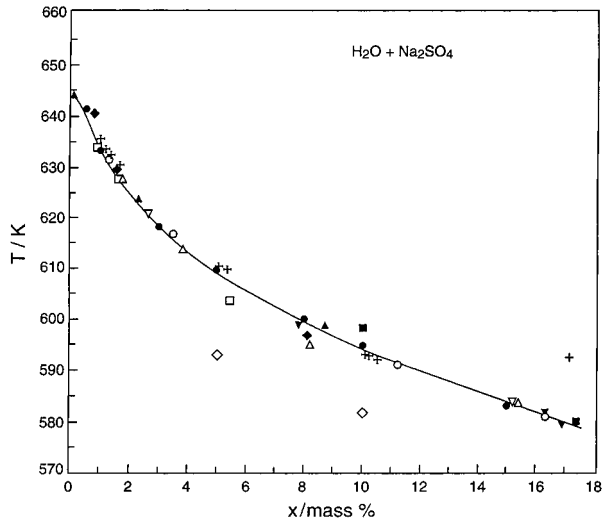

Figure 7. Temperature−composition plot for the liquid at the three-phase equilibrium. The solid curve is a guide to the eye. +, Smits;[6] ▽, Schroeder et al.;[23,24] ▼, Benrath et al.;[25] ◇, Benrath;[26] ◆, Keveel;[27] □, Booth et al.;[28] ■, Ravich et al.;[29] △, Marshall et al.;[30] ▲, Zdanovsky;[19] ○, Khaibullin and Novikov;[3] ●, Khaibullin and Novikov;[4] cross, this work.

overriding source of uncertainty in the composition is that in the liquid and vapor densities. As explained above, the uncertainties in composition were obtained by allowing maximum offsets for liquid and vapor densities.

Figure 7 shows the compositions of liquid solutions in the three-phase equilibrium (L−G−S), plotted using all available literature data, namely those in the compilation of Zdanovsky et al.[19] referred to in the figure caption, plus those of Kh.[3,4] It is seen that our solubility data differ from the averaged solubility curve by no more than ±0.5 mass % Na_2SO_4 at 590 K to 610 K, and by less than ±0.25 mass % at 630 K to 634 K. If it is taken into account that most of the high-temperature solubility data in the literature were obtained with an uncertainty of about ±0.5 mass %, the agreement of the new values with the available experimental data is quite satisfactory.

Density and Composition of the Liquid at the Three-Phase Line as the Vapor Phase Disappears

There are five isochores for which the second peak disappears in the range below 640 K, the highest temperature for which there are Kh[3,4] data on the three-phase line. They are the ones listed in Table 3 with transition temperatures of 598.55 K, 603.58 K, 615.83 K, 619.62 K, and 638.24 K, respectively.

In case 3, first peak, the Kh[3,4] liquid and vapor densities were accepted and used to calculate the composition of the liquid. In case 3, second peak, the liquid occupies the entire volume, except for the small space occupied by the solid, for which the density is known but the volume needs to be calculated. For Na_2SO_4, the specific volume $V_{spec,\,sol}$ is taken as (2.7 ± 0.1) $cm^3 \cdot g^{-1}$, and that of Na_2CO_3, to be discussed later, is taken as (2.5 ± 0.1) $cm^3 \cdot g^{-1}$. The analogue of eqs 2−4 could have been obtained by replacing vapor density and volume by solid density and volume. In this case, however, M and $V\rho_{liq}$ are almost the same, so given the limited accuracy of the Kh[4] densities, one cannot expect to obtain the volume occupied by the solid with any reliability at all from the analogue of eq 3. Instead, we interpolated the liquid mass % composition from the composite three-phase $T-x$ curve at the transition temperature (Figure 7) and calculated the liquid density from the amount of salt dissolved, $M_{salt,diss}$, the amount and hence volume of solid salt, V_{sol}, and the volume of liquid, $V - V_{sol}$, as follows:

$$x_{liq}/100 = M_{salt,diss}/(M_w + M_{salt,diss}) \quad (5)$$

$$V_{sol} = (M - M_{salt,diss})V_{spec,sol} \quad (6)$$

$$\rho_{sol}V_{sol} + \rho_{liq}(V - V_{sol}) = M \quad (7)$$

$M_{salt,diss}$ is calculated from x_{liq} through eq 5, V_{sol} from eq 6, and ρ_{liq} from eq 7. The calculation was done twice, namely, for the extreme values the various properties assume given their uncertainties: that of the solubility on the three-phase curve, ±10% of solubility; that of the volume of the calorimeter, ±0.05%; and that of the specific volume of the salt, ±0.1 $cm^3 \cdot g^{-1}$. The average liquid densities and their uncertainties are listed in the "density" column for the liquid in Table 3.

As an example, consider the 10 mass % second peak at 619.62 K, for which the properties are T_{trans} = (619.62 ± 0.19) K, M_{salt} = 7.079, $V_{spec,sol}$ = (2.7 ± 0.1) $cm^3 \cdot g^{-1}$, $V(P,T)$ = (103.18 ± 0.05) cm^3, M_{water} = 63.713 g, x_{liq} = (2.8 ± 0.28) mass %, and M = 70.792 g. The highest value of the solid solubility is (2.8 + 0.28)% = 3.08 mass %. This will yield the lowest solid volume and the highest liquid density. Thus, 2.025 g of salt must be dissolved in 63.713 g of water. Then 5.054 g of salt is deposited, with a volume of minimally 1.940 and maximally 1.944 cm^3. The minimum liquid volume is the minimum of the cell volume, 103.13 cm^3, minus the maximum of the salt volume, 1.944 cm^3, leading to 101.186 cm^3. This yields a maximum liquid density of 0.6497 $g \cdot cm^{-3}$. The calculation is repeated for the minimum solubility, 2.52 mass %, which combined with the maximum cell volume, 103.23 cm^3, yields 0.6453 $g \cdot cm^{-3}$ for the liquid density. The value listed in Table 3, 647.5 $kg \cdot m^{-3}$, is the average of the two extremes, and the uncertainty, 2.2 $kg \cdot m^{-3}$, is half of the largest spread. Thus, by assuming that the composite $T-x$ curve is accurate to ±10% in solubility, we have been able to obtain new liquid density values on the three-phase curve, with uncertainties from (2.2 to 5.4) $kg \cdot m^{-3}$.

A composite $T-\rho$ plot is shown in Figure 8. The four new densities agree with the Kh[4] ones to within a combined uncertainty.

Disappearance of a Fluid Phase in the Presence of Solid above 640 K

Far from criticality, the second peak, corresponding to disappearance of vapor in three-phase equilibrium, looks very similar to the "jumps" of $T-C_{vx}$ curves at the phase transition L−G ⇔ L. Closer to criticality, however, the slope of the C_{vx} versus temperature curve becomes steeper. Therefore, the temperature range corresponding to the "jump" of C_{vx} values, or to the peak just beyond the transition, was used as a characteristic for the sharpness, or the uncertainty in temperature, of the phase transition.

The shape of the second peak is λ-like, no matter whether it is the liquid (case 3, second peak) or gas phase (case 4, second peak) that disappears in the vicinity of the critical end point.

The temperature of the critical end point corresponds to the temperature maximum of the three-phase equilibrium, at which point the compositions, densities, and other properties of equilibrium saturated liquid and vapor solutions become identical. If the temperature dependence of any suitable property is known in both the liquid and vapor phases, the temperature can be located where these two

Table 4. Densities of Liquid and Vapor Solutions in Three-Phase Equilibrium for the System $Na_2CO_3 + H_2O$ near the Critical End Point

init conc (mass %)/ avg density ($kg \cdot m^{-3}$)	T/K	liquid solution Na_2CO_3		vapor solution Na_2CO_3	
		x/mass %	ρ/kg.m^{-3}	x/mass %	ρ/kg·m^{-3}
5/412.13	647.19 ± 0.16	<0.3	388.0 ± 0.8		
5/371.60	648.68 ± 0.14	<0.3	349.7 ± 0.8		
5/299.72	648.95 ± 0.10			<0.3	281.7 ± 0.6
5/245.52	648.32 ± 0.17			<0.3	230.5 ± 0.5

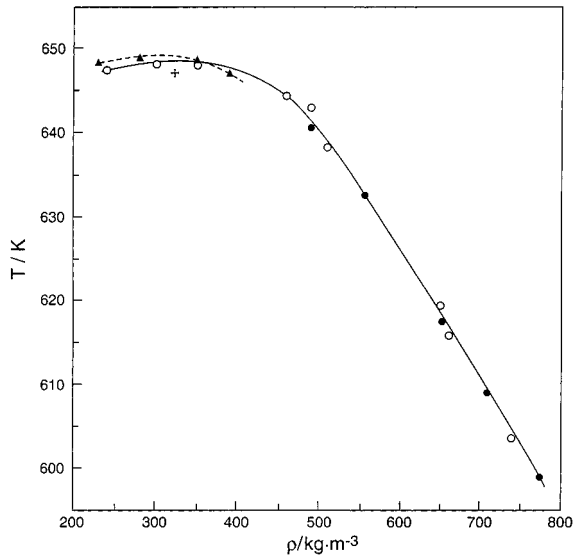

Figure 8. Temperature dependence of the density of the fluid on the three-phase curve up to the critical end point for aqueous sodium sulfate and sodium carbonate. The critical end point temperatures exceed the critical point of water by about 1 K. Aqueous Na_2SO_4: O, this work, from C_{vx}; ●, Khaibullin and Novikov,[4] from $PVTx$. Aqueous Na_2CO_3: ▲, this work and Abdulagatov et al.,[4] from C_{vx}; cross, pure water.[31] Solid curve: guide to the eye for aqueous Na_2SO_4. Dashed curve: guide to the eye for aqueous Na_2CO_3.

property values become equal. In the present case, the solution density is the property of choice. To calculate this density, however, it is necessary to know the solubility, because a large fraction of the salt originally present in the solution has already precipitated due to the negative temperature coefficient of solubility of Na_2SO_4. Experimental solubility data, however, are available only up to 640.5 K, where the concentration of saturated liquid solution is 0.5 mass % Na_2SO_4. The present experimental data show, however, that the three-phase equilibrium (L−G−S) exists at higher temperatures, where the concentration of equilibrium solutions must be lower than 0.5 mass % Na_2SO_4.

In first approximation, it is assumed that all salt was crystallized. In this case the density of the remaining water can be easy calculated from the measured mass of water and the volume of the calorimeter minus that of the solid salt. Then, similar calculations can be made if the concentration of solution is assumed to equal 0.3 mass % Na_2SO_4. The results of calculation show that the variations in the values of density are only a few kilograms per cubic meter. That means that the uncertainty in our density values is less than 1%. The liquid or vapor densities nearest to the critical end point are listed in the last five lines of Table 3.

As an example, consider the first point on the gas side in Table 1, which is the last point listed in Table 3. This point is characterized by an overall density of 250.1 $kg \cdot m^{-3}$ with $T_{trans} = (647.42 \pm 0.35)$ K, $M_{salt} = 0.254$ g, $V_{spec,sol} = (2.7 \pm 0.1)$ cm$^3 \cdot$g^{-1}, $V(P,T) = (103.34 \pm 0.05)$ cm^3, $M_{water} = 25.119$ g, $P(Kh,T) = 22.1$ MPa, and $M = 25.373$ g.

If it is assumed that no salt is dissolved, the solid volume is a minimum of 0.091 cm^3 and a maximum of 0.098 cm^3. The fluid volume then is a maximum of 103.39−0.091 = 103.30 cm^3. Likewise, the minimum volume equals 103.29 − 0.098 = 103.19 cm^3. The fluid density then ranges from 25.119/103.30 = 243.2 $kg \cdot m^{-3}$ to 25.119/103.19 = 243.4 $kg \cdot m^{-3}$.

If it is assumed that the solubility equals 0.3 mass %, then 0.076 g of salt is dissolved in 25.119 g of water, and 0.178 g of salt is not dissolved. The mass of the fluid is 25.195 g. The volume occupied by the undissolved salt ranges from 0.064 cm^3 to 0.068 cm^3. Thus, the volume available to the fluid phase ranges from 103.39 − 0.064 = 103.33 cm^3 to 103.29−0.068 = 103.22 cm^3. The density then ranges from 243.8 $kg \cdot m^{-3}$ to 244.1 $kg \cdot m^{-3}$. An uncertainty of 1 mg in the mass of salt would not have affected the results significantly. The fluid density thus ranges from 2.432 to 2.441 $kg \cdot m^{-3}$. The values obtained for the densities are listed in Table 3; they represent the average of the two extreme values for 0 mass % salt and 0.3 mass % salt. The uncertainties listed represent half the spread. These particular near-critical densities are thus quite well-known indeed, to about 0.3%.

In Figure 8, the density of the fluid along the three-phase curve is plotted up to the highest measured temperatures. Of the five densities above 640 K, only the lowest one, at 643 K, appears to be an outlier. The other four define a smooth curve, with a temperature maximum at (648.2 ± 0.2) K, the uncertainty being that of the transition temperatures for the nearest points; see Table 3. This maximum corresponds to the first critical end point, where the densities of liquid and vapor solutions in the three-phase equilibrium become identical. The critical end point is located about 1 K above the water critical point, the latter estimated to be (647.1 ± 0.1) K by Levelt Sengers et al.[31,32] Values of the critical temperature of pure water observed after 1975 by various experimenters in the Dagestan Laboratory tend to fall near the high end of this same range; see Abdulagatov et al.[32,33]

In the same figure, four values are shown of the density of the liquid or vapor solution of Na_2CO_3 in three-phase equilibrium. The latter data show a similar $T-\rho$ curve with a maximum at the first critical end point, which occurs at a temperature of (649.0 K ± 0.2) K, almost 2 K above the water critical point. The experimental data for these points were taken from the $T-C_{vx}$ isochores at the fill densities 245.52 $kg \cdot m^{-3}$, 299.72 $kg \cdot m^{-3}$, 371.60 $kg \cdot m^{-3}$, and 412.13 $kg \cdot m^{-3}$ for 5 mass % Na_2CO_3 of Abdulagatov et al.[2] The densities of solutions on the three-phase curve around the critical end point were estimated by the same method as was described above for subcritical solutions of Na_2SO_4. The results are summarized in Table 4 and Figure 8.

The data in Figure 8 do not allow any firm conclusion on the critical end point densities in these two systems, other than that they are not clearly different from that of pure water.

Conclusions

On isochoric heating, heat capacity data for aqueous sodium sulfate and aqueous sodium carbonate show features such as jumps and spikes, which indicate the occurrence of phase transitions. In the present systems, these transitions are the appearance of a solid phase, the disappearance of a vapor or a liquid phase, and near-critical transitions. The appearance of a solid phase is accompanied by hysteresis effects. A method has been developed in order to correct for these effects. The corrected transition points are generally in good agreement with those obtained from the Khaibullin−Novikov *PVTx* data. The densities presented here for liquid solutions are more accurate than those hitherto available. The near vicinity of the critical end points in aqueous Na_2SO_4 and Na_2CO_3 systems has been probed. The present data allow, for the first time, us to distinguish the critical end point temperature of these salt solutions from the critical temperature of water. This paper demonstrates that isochoric heat capacity data of the type reported here are a very sensitive tool for determining the location of fluid- and solid-phase boundaries of fluids and fluid mixtures. This kind of information is crucial in designing chemical processes in supercritical processes, where formation of solids could plug the apparatus.

Since overall composition and density along the isochore are carefully measured, the fluid mixture density, an elusive quantity in most engineering phase equilibria measurements, can be accurately determined at the point that a vapor phase disappears in the absence of solid.

To interpret transitions from two to three phases, and calculate fluid properties on a three-phase line, information from an independent source is needed. Then, the heat capacity data can be used to check the consistency of literature data.

Near the end of the three-phase line, where the solid solubility is very low, the isochoric heat capacity data can be used to calculate the density of the liquid or the vapor as the other phase disappears. Again, these are data very hard to obtain by any other means.

It should be very interesting to perform isochoric heat capacity measurements in a binary aqueous system in which the L1−L2−G three-phase line is not totally suppressed by the solid, as it is in the present cases.

Literature Cited

(1) Abdulagatov, I. M.; Dvorayanchikov, V. I.; Mursalov, B. A. Vapor−Liquid−Solid Phase Transitions in Aqueous Sodium Sulfate and Sodium Carbonate from Heat Capacity Measurements near the First Critical End Point. 1. Sodium Sulfate Data *J. Chem. Eng. Data* **2000**, *45*, 1133.

(2) Abdulagatov, I. M.; Dvoryanchikov, V. I.; Mursalov, B. A.; Kamalov, A. N. Heat capacity at constant volume of H_2O+Na_2CO_3 solutions near the critical point of pure water. *J. Solution Chem.* **1999**, *28*, 871−889.

(3) Khaibullin, I. Kh.; Novikov, B. E. A thermodynamic study of aqueous and steam solutions of sodium sulfate at high temperatures. *Teplofiz. Vys. Temp.* **1973**, *11*, 320−327. English translation: *High Temp.* **1973,** *11*, 276−282.

(4) Khaibullin, I. Kh.; Novikov, B. E. Experimental determination of saturated solution conditions at high temperatures with a method of gamma-rays. *Teplofiz. Vys. Temp.* **1972**, *10*, 895−897. English translation: *High Temp.* **1973,** *10*, 805−807.

(5) Étard, M. A. État des sels dans les solutions; sulfate de sodium et chlorure de strontium. *Comptes Rendus* **1891**, *113*, 854−857.

(6) Smits, A.; Wuite, J. P. On the system water-natrium sulphate. *Proc. K. Ned. Akad. Wet.* **1909**, 12, 244−257.

(7) Sharygin, A. V.; Mokbel, I.; Xiao, C.; Wood, R. H. In preparation for *J. Phys. Chem.*

(8) Buechner, E. H. Die beschränkte Mischbarkeit von Flüssigkeiten; das System Diphenylamin und Kohlensaüre. *Z. Phys. Chem.* **1906,** *56*, 257−318.

(9) Buechner, E. H. *Die Heterogenen Gleichgewichte vom Standpunkte der Phasenlehre von H. W. Bakhuis Roozeboom*, 2ter Teil, *Systeme Mit Zwei Flüssigen Phasen*; 2tes Heft, *Systeme Aus Zwei Komponenten*; Braunschweig: 1918.

(10) Smits, A. The course of solubility in the region of the critical temperatures of binary mixtures I. *Proc. K. Ned. Akad. Wet.* **1903**, *7*, 171−181.

(11) Smits, A. The course of solubility in the region of the critical temperatures of binary mixtures II. *Proc. Kon. Ned. Akad. Wet.* **1904**, *8*, 484−497.

(12) Smits, A. Die P,T,x-Raumdarstellung vom System Aether-Antrachinon, *Z. Phys. Chem.* **1911**, *76*, 445−449.

(13) Van Konynenburg, P. H.; Scott, R. L. Critical lines and phase equilibria in binary van der Waals mixtures. *Philos. Trans. R. Soc. London* **1980**, *298*, 495−540.

(14) Valyashko, V. M. *Phase Equilibria and Properties of Hydrothermal Solutions;* Nauka: Moscow, 1990.

(15) Valyashko, V. M. Phase behavior in binary and ternary water-salt systems at high temperatures and pressures. *Pure Appl. Chem.* **1997**, *69*, 2271−2280.

(16) Peters, C. J. Multiphase equilibria in near-critical solvents. In *Supercritical Fluids, Fundamentals for Application*; Kiran, E., Levelt Sengers, J. M. H., Eds.; NATO ASI Series 273; Kluwer Academic Publishers: Dordrecht, 1994; pp 117−145.

(17) Griffiths, R. B.; Wheeler, J. C. Critical points in multicomponent systems. *Phys. Rev.* **1970**, *A2*, 1047−1064.

(18) Anisimov, M. A.; Voronel, A. V.; Gorodetskii, E. E. Isomorphism of critical phenomena. *Sov. Phys. JETP* **1971**, *33*, 605−612.

(19) Zdanovsky, A. B.; Solov'eva, E. F.; Ezrokhi, L. L.; Lyakhovskaya, E. I. *Data book on experimental data on solubility in water-salt systems.* III; Vyazovov, V. V., Pel'sh, A. D., Eds.; Gos. Izdat. Khim. Literat.: Leningrad, 1962.

(20) Taylor, B. N.; Kuyatt, C. E. Guidelines for evaluating and expressing the uncertainty of NIST measurement results. NIST Technology Note 1297; U.S. Government Printing Office: Washington, DC, 1994.

(21) Harvey, A. H.; Peskin, A. P.; Klein, S. A. *NIST/ASME Steam Properties*, NIST Standard Reference Database 10, Version 2.1; Standard Reference Data Program, NIST: Gaithersburg, MD, 1997.

(22) Harvey, A. H.; Bellows, J. C. *Evaluation and Correlation of Steam Solubility Data for Salts and Minerals of Interest in the Power Industry*. NIST Technical Note 1387; U.S. Government Printing Office: Washington, DC, 1997.

(23) Schroeder, W. C.; Gabriel, A. Solubility equilibria of sodium sulfate at temperatures from 150 to 350 °C. *J. Am. Chem. Soc.* **1935**, *57*, 1539−1546.

(24) Schroeder, W. C.; Berk, A. A.; Gabriel, A. Solubility equilibria of sodium sulfate at temperature from 150 to 350 °C. III. Effect of sodium hydroxide and sodium phosphate. *J. Am. Chem. Soc.* **1937**, *59*, 1783−1790.

(25) Benrath, A.; Gjedebo, F.; Schiffers, B.; Wunderlich, H. Über die Löslichkeit von Salzen und Salzgemischen in Wasser bei Temperaturen oberhalb von 100 °C. I. *Z. Anorg. Allg. Chem.* **1937**, *231*, 285−297.

(26) Benrath, A. Über die Löslichkeit von Salzen und Salzgemischen in Wasser bei Temperaturen oberhalb von 100 °C. *Z. Anorg. Allg. Chem.* **1941**, *247*, 147−160.

(27) Keveel, N. B. Vapor pressure of aqueous solutions at high temperatures. *J. Am. Chem. Soc.* **1942**, *64*, 841−850.

(28) Booth, H. S.; Biswell, R. M. Solubilities of salts in water at high temperatures. *J. Am. Chem. Soc.* **1950**, *72*, 2567−2575.

(29) Ravich, M. I.; Borovaya, F. E.; Ketkovich, V. Ya. Solubility and vapor pressure of saturated solutions in the system NaCl−Na_2SO_4−H_2O at high temperatures. *Izv. Sekt. Fiz.-Khim. Anal.* **1953**, *22*, 240−254.

(30) Marshall, W. L.; Wright, H. W.; Secoy, C. H. A phase-study apparatus for semi-micro use above atmospheric pressure. *J. Chem. Educ.* **1954**, *31*, 34−36.

(31) Levelt Sengers, J. M. H.; Straub, J.; Watanabe, K.; Hill, P. G. Assessment of critical parameter values for H_2O and D_2O. *J. Phys. Chem. Ref. Data* **1985**, *14*, 193−207. The revised values, on ITS-90, can be found in: *Physical Chemistry of Aqueous Systems;* White, H. J., Jr., Sengers, J. V., Neumann, D. B., Bellows, J. C., Eds.; Begell House: New York, 1995; Appendix A101−A102.

(32) Abdulagatov, I. M.; Dvoryanchikov, V. I.; Kamalov, A. N. Heat capacity at constant volume of pure water in the temperature range 412−693 K at densities from 250 to 925 kg m^{-3}. *J. Chem. Eng. Data* **1998**, *43*, 830−838.

(33) Abdulagatov, I. M.; Magee, J.; Friend, D.; Kiselev, S. A critical assessment of experimental data and correlation for heat capacity at constant volume of water and steam. *J. Phys. Chem. Ref. Data*, in preparation.

Received for review April 27, 2000. Accepted August 22, 2000. CRDF Award Number RP1-358 and RFBR Project 97-03-33274 enabled the participation of V.M.V at NIST. V.M.V. also thanks W.S. Hurst and A. Lee for hospitality and encouragement. The experimental work was supported by INTAS Grant No. INTAS-96-1989. Two of us (V.M.V. and I.M.A.) acknowledge the hospitality of the Division of Physical and Chemical Properties at NIST. J.M.H.L.S. is grateful for the hospitality of the Instituut voor Theoretische Fysica, University of Utrecht, Netherlands, where part of the paper was written.

JE000123Z